



Received 9 December 2019
Accepted 6 January 2020

Edited by A. Van der Lee, Université de Montpellier II, France

Keywords: crystal structure; $\text{AgSr}_4\text{Cu}_{4.5}(\text{PO}_4)_6$; transition metal phosphate; hydrothermal synthesis; layered structure.

CCDC reference: 1975726

Supporting information: this article has supporting information at journals.iucr.org/e

Crystal structure of silver strontium copper orthophosphate, $\text{AgSr}_4\text{Cu}_{4.5}(\text{PO}_4)_6$

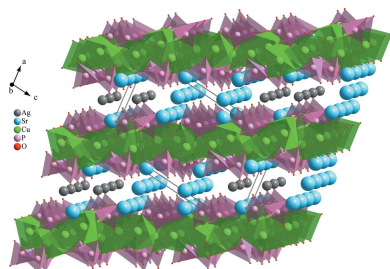
Jamal Khmiyas,* Elhassan Benhsina, Said Ouaatta, Abderrazzak Assani, Mohamed Saadi and Lahcen El Ammari

Laboratoire de Chimie Appliquée des Matériaux, Centre des Sciences des Matériaux, Faculty of Sciences, Mohammed V University in Rabat, Avenue Ibn Batouta, BP 1014, Rabat, Morocco. *Correspondence e-mail: j_khmiyas@yahoo.fr

Crystals of the new compound, $\text{AgSr}_4\text{Cu}_{4.5}(\text{PO}_4)_6$, were grown successfully by the hydrothermal process. The asymmetric unit of the crystal structure of the title compound contains 40 independent atoms (4 Sr, 4.5 Cu, 1 Ag, 6 P and 24 O), which are all in general positions except for one Cu atom, which is located on an inversion centre. The Cu atoms are arranged in CuO_n ($n = 4$ or 5) polyhedra, linked through common oxygen corners to build a rigid three-dimensional motif. The connection of these copper units is assured by PO_4 tetrahedra. This arrangement allows the construction of layers extending parallel to the (100) plane and hosts suitable cavities in which Ag^+ and Sr^{2+} cations are located. The crystal-structure cohesion is ensured by ionic bonds between the silver and strontium cations and the oxygen anions belonging to two adjacent sheets. Charge-distribution analysis and bond-valence-sum calculations were used to validate the structural model.

1. Chemical context

The growing role of metal orthophosphates based on PO_4 and MO_n (where M is a metal cation) structural units is closely related to their ability to adopt different spatial arrangements. As has been pointed out previously, their physical and chemical properties, dynamic flexibility attributes and structural behaviour (Hadrich *et al.*, 2001) can be correlated with the ionic radius of the metal cation (Jeżowska-Trzebiatowska *et al.*, 1980). Furthermore, the ability of these metal cations to adopt different oxidation states as well as various coordination environments leads, in general, to open anionic three-dimensional frameworks. The structures of these classes of materials can easily accommodate a great variety of substituents, anionic and/or cationic, which can have a significant effect on the stability and on the morphology of structures and crystals, as is shown particularly in the apatite family (LeGeros & Tung, 1983) for which a considerable number of complex and versatile networks were described systematically. Open frameworks involved with various cavities such tunnels or cages, especially in phosphates containing mono, di and trivalent cations, are of particular interest owing to their potential applications in catalysis (Badrour *et al.*, 2001) and as immobilizing carriers for various enzymes, *e.g.* $\text{CaTi}_4(\text{PO}_4)_6$ (Suzuki *et al.*, 1991) as well as for their photocatalytic activities in glass-ceramics containing $\text{MgTi}_4(\text{PO}_4)_6$ crystals (Fu, 2014) and ionic-conductivity properties with $\text{Ca}_{1-x}\text{Na}_{2x}\text{Ti}_4(\text{PO}_4)_6$ belonging to the Nasicon structure type (Mentre & Abraham, 1994). Much attention has been paid to compounds containing six PO_4 tetrahedral units with different transition metal/phosphate ratios, *e.g.* $\text{Na}_4\text{CaFe}_4(\text{PO}_4)_6$ which adopts the

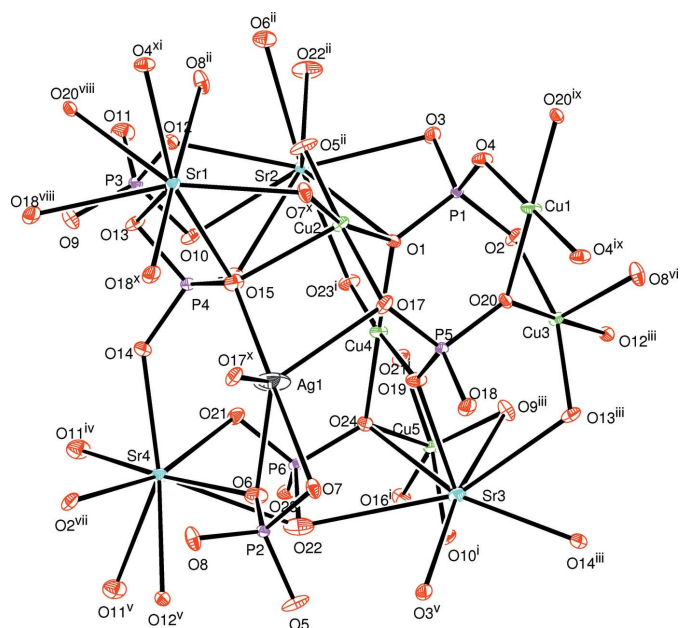


OPEN ACCESS

Alluaudite structure in the ideal $C2/c$ space group (Hidouri *et al.*, 2004), $\text{Ba}_3\text{V}_4(\text{PO}_4)_6$ which crystallizes as a Langbeinite-type structure (Dross & Glaum, 2004), $\text{CuTi}_4(\text{PO}_4)_6$ which belongs to the Nasicon family (Kasuga *et al.*, 1999), the silver lead apatite $\text{Pb}_8\text{Ag}_2(\text{PO}_4)_6$ (Ternane *et al.*, 2000), the mixed-valent iron(II/III) phosphate $\text{Fe}_7(\text{PO}_4)_6$ (Belik *et al.*, 2000) and $\text{Na}_{2.5}\text{Y}_{0.5}\text{Mg}_7(\text{PO}_4)_6$ with a Fillowite-type structure (Jerbi *et al.*, 2010). Through hydrothermal processes, and as part of our systematic studies of the crystal alkaline and alkaline earth monophosphates, we have previously succeeded in elaborating a number of compounds with three-dimensional networks featuring distinctive cavities including $\text{AgMg}_3(\text{HPO}_4)_2\text{PO}_4$ (Assani *et al.*, 2011), $\text{Sr}_2\text{Mn}_3(\text{HPO}_4)_2(\text{PO}_4)_2$ (Khmiyas *et al.*, 2013), $\text{SrMn}_2^{\text{II}}\text{Mn}^{\text{III}}(\text{PO}_4)_3$ (Alhakmi *et al.*, 2013), $\text{NaMg}_3(\text{HPO}_4)_2\text{PO}_4$ (Ould Saleck *et al.*, 2015). In an extension of our investigations and structural studies of various mono-divalent transition-metal phosphates a new phosphate copper (Cu^{II})-based $\text{AgSr}_4\text{Cu}_{4.5}(\text{PO}_4)_6$ was prepared and successfully characterized. Charge-distribution (CHARDI) (Nespolo *et al.*, 2001) and bond-valence-sum (BVS) calculations were used for validating the structural model. A careful examination of the literature as well as various databases reveals that the title compound $\text{AgSr}_4\text{Cu}_{4.5}(\text{PO}_4)_6$ is original and furthermore is not related to any family of reported compounds.

2. Structural commentary

The principal building units of the crystal structure of $\text{AgSr}_4\text{Cu}_{4.5}(\text{PO}_4)_6$ are more or less distorted polyhedra (AgO_5 , CuO_4 , CuO_5 , SrO_8 , SrO_9) and nearly regular PO_4 tetrahedra,



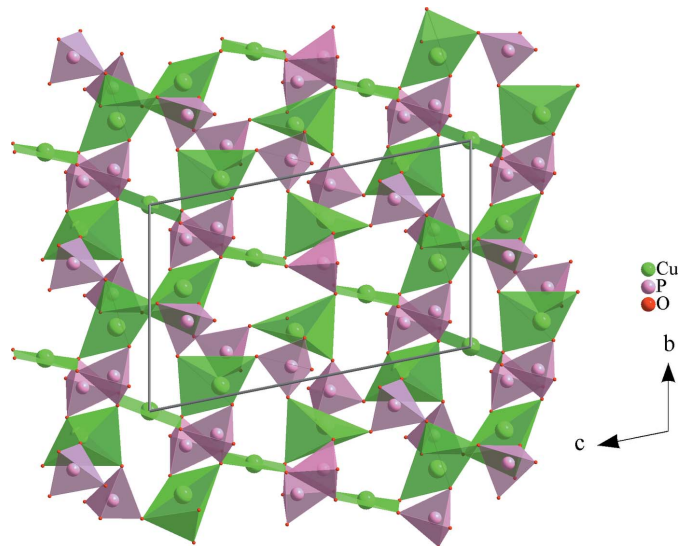


Figure 5
A $[\text{Cu}_3\text{O}_{12}]$ trimer linked to PO_4 through corners to form a layer parallel to the (100) plan.

first trimer results from the zigzag succession in the following order $\text{Cu}(4)\text{O}_5 - \text{Cu}(2)\text{O}_4 - \text{Cu}(5)\text{O}_5$. Similarly, the second type of trimer is built up from two-vertex-sharing of a single polyhedra, Cu_1O_4 , sandwiched by two neighbouring Cu_3O_5 entities as shown in Fig. 2. Each oxygen atom of both trimers is connected to a nearly regular PO_4 tetrahedron in such a way as to form two different $[\text{Cu}_3\text{P}_{10}\text{O}_{40}]^{24-}$ ribbons (see Fig. 3 and 4). These adjacent ribbons are linked together through the PO_4 tetrahedra, thus building a layer-like $[\text{Cu}_{4.5}(\text{PO}_4)_6]^{10-}$ arrangement perpendicular to the [100] direction as shown in Fig. 5.

Crystal cohesion and the junction between the stacked layers along the a -axis direction are ensured by ionic bonds involving the Sr^{2+} and Ag^+ cations as shown in Fig. 6. The insertion of these mono and bivalent cations generates strong interactions inducing, consequently, a morphological deforma-

mation of the interlayer space, which explains the manifestation of the distorted sites. This result is confirmed by the CHARDI analysis of the coordination polyhedra by means of the effective coordination number (ECoN; Nespolo, 2016). The distortion of the metal–oxygen polyhedron becomes stronger when the ECoN value deviates further from the habitual coordination number (CN). This structural particularity is clearly noticeable when examining the numerical values of ECoN and CN for the various SrO_n ($n = 8$ and 9) and AgO_5 polyhedra. The differences $\text{ECoN}(\text{Sr}1)/\text{CN}(\text{Sr}1) = 7.61/8$, $\text{ECoN}(\text{Sr}2)/\text{CN}(\text{Sr}2) = 6.96/8$ and $\text{ECoN}(\text{Sr}3)/\text{CN}(\text{Sr}3) = 6.8/8$, reveal an increased distortion in the SrO_8 groups ranging from the $\text{Sr}1\text{O}_8$ to $\text{Sr}3\text{O}_8$ polyhedra. The $\text{Sr}2$ atom is formally nine-coordinate with bond lengths varying from 2.480 (2) to 2.890 (2) Å. The site hosting $\text{Sr}4$ is very flexible and bulky, resulting in a greatly deformed SrO_9 polyhedron. The geometry ratio $\text{ECoN}(\text{Ag}1)/\text{CN}(\text{Ag}1) = 3.93/5$ of the AgO_5 polyhedron indicates a distorted square-pyramidal coordination environment. This behaviour can be attributed to the edge or face-sharing between these polyhedral units. This modality of linkage, as well as the ionic radius of Sr^{2+} and Ag^+ , induces a strong cation–cation electrostatic repulsion, which is reflected in the interatomic distances and consequently on the repetition of the ionic charge and bond-valence-sum (BVS) values.

The CHARDI analysis method gives the distribution of calculated ECoN numbers of a central cation among all the neighbouring anions (Hoppe, 1979). The calculation of this number is related directly to the distribution of charges in crystalline structures. The measure of the correctness of the structure (cation ratio) and of the degree of over or under bonding (anion ratio) is performed *via* the evaluation of the internal criterion q/Q (where q is the formal oxidation number and Q the computed charge). The charge-distribution method (CD or CHARDI), developed by Hoppe *et al.* (1989), and the bond–valence (BVS) approach introduced to predict bond lengths in inorganic crystals (Brown, 1977, 1978) provide powerful tools for analysis of the connectivity of crystal structures and the validation of structural models. In the present study, both validation tools, BVS and CHARDI, are applied to the structural model of the title compound. Generally, for a well-refined structure, the calculated valences $V(i)$ obtained by the BVS model and the computed charge $Q(i)$ according to the CHARDI analysis must be in close agreement with the oxidation number of the atoms. The CHARDI computations were carried out with the CHARDI2015 program (Nespolo & Guillot, 2016), while BVS was calculated using PLATON (Spek, 2009). In the asymmetric unit, all atoms are located on general positions (Wyckoff position 2*i*) of space group $P\bar{1}$ except for Cu1, which is located on a special position (Wyckoff position 1*a*). The distribution of the electric charges at the 40 crystallographic sites of the asymmetric unit shows that the Ag^+ , Sr^{2+} , Cu^{2+} and P^{5+} cations fully occupy 16 sites. Otherwise, charge neutrality requires the location of 24 oxygen atoms in the remaining 2*i* sites. The first results of BVS calculations for Sr3 suggest a valence $V(\text{Sr}3) = 1.900$ v.u. for a coordination number $\text{CN} = 7$.

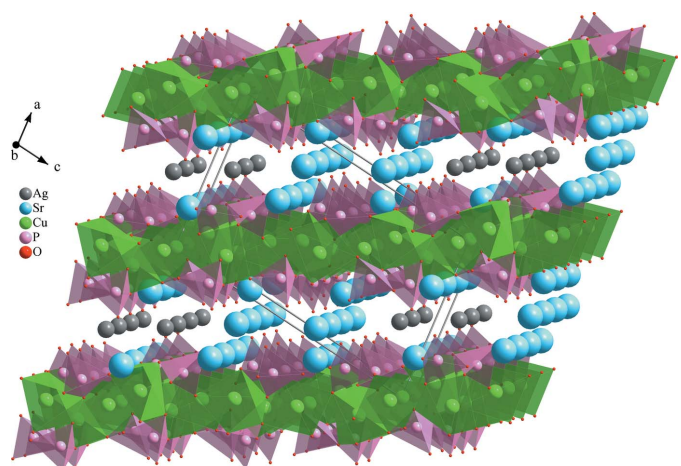


Figure 6
Three dimensional view of $\text{AgSr}_4\text{Cu}_{4.5}(\text{PO}_4)_6$ crystal structure showing Sr^{2+} and Ag^+ between layers stacked along the [100] direction.

Table 1

CHARDI and BVS analysis for the cations in the title compound.

$q(i)$ = formal oxidation number; $\text{sof}(i)$ = site occupancy; $\text{CN}(i)$ = classical coordination number; $Q(i)$ = calculated charge; $V(i)$ = calculated valence; $\text{ECoN}(i)$ = effective coordination number.

Cation	$q(i)\cdot\text{sof}(i)$	$\text{CN}(i)$	$\text{ECoN}(i)$	$V(i)$	$Q(i)$	$q(i)/Q(i)$
Ag1	1	5	3.93	0.998	1.02	0.98
Sr1	2	8	7.61	2.125	2.03	0.98
Sr2	2	8	6.96	2.308	1.99	1.00
Sr3	2	8	6.80	1.962	1.98	1.01
Sr4	2	9	8.07	2.248	2.01	0.99
Cu1	2	4	3.97	1.765	1.92	1.04
Cu2	2	4	3.97	2.000	1.96	1.02
Cu3	2	5	4.55	2.050	1.94	1.03
Cu4	2	5	4.37	2.039	2.00	1.00
Cu5	2	5	4.25	1.957	1.94	1.03
P1	5	4	3.97	4.892	4.91	1.02
P2	5	4	4.00	4.962	5.20	0.96
P3	5	4	3.97	4.974	4.98	1.00
P4	5	4	3.99	4.944	5.04	0.99
P5	5	4	3.97	4.939	4.93	1.01
P6	5	4	3.99	5.016	5.10	0.98

This result can be significantly improved by widening the coordination sphere to 3.1410 \AA , which allows the integration of a supplemental oxygen, thus inducing valence $V(\text{Sr}3) = 1.962$ v.u. The analysis of the data summarized in Table 1 reveals that the values obtained from charges $Q(i)$ and bond-valence sums $V(i)$ of the cations are all compatible with the weighted oxidation number $q(i)\cdot\text{sof}(i)$. The minor deviations reported from these parameters with respect to the formal oxidation state are closely related to the distortion level of the occupied sites. Despite these irregularities, all the values of the internal criterion $q(i)/Q(i)$ are very close to unity, which confirms the validity of the structural model obtained from the X-ray diffraction data. The convergence of the CHARDI model is evaluated by the mean absolute percentage deviation (MAPD) as shown in the equation below, which measures the agreement between $q(i)$ and $Q(i)$ for the whole sets of PC atoms (polyhedron-centring atoms) and of V atoms (the vertex atoms) (Eon & Nespolo, 2015). For the cationic charges in the structure, we report that the calculated value of MAPD is only 1.7%.

$$\text{MAPD} = \frac{100}{N} \sum_{i=1}^N \left| \frac{q(i) - Q(i)}{q(i)} \right|$$

where N is the number of polyhedron-centring or vertex atoms in the asymmetric unit.

The calculated anionic charges $Q(i)$ of oxygen show a lowest deviation of the order of 4.5% with respect to $q(i)$. These values of MAPD show that the dual description as cation-centred and anion-centred is satisfactory and adequate for the studied structural model. The ratio $q(i)/Q(i)$ is approximately equal to 1 in most cases (Table 2), with some exceptions: $q(O8)/Q(O8) = 1.16$, $q(O12)/Q(O12) = 0.92$ and $q(O22)/Q(O22) = 1.15$. This anomaly of negative-charge repetition could be due to the OUB effect (over-under bonding effect) (Nespolo *et al.*, 1999), which results from the repulsive interactions of the cations located at the centre of

Table 2

CHARDI calculation for the oxygen anions in the title compound.

Atom	$\text{sof}(i)$	$q(i)$	$Q(i)$	$q(i)/Q(i)$
O1	1	-2	-2.02	0.99
O2	1	-2	-2.07	0.97
O3	1	-2	-1.98	1.01
O4	1	-2	-2.08	0.96
O5	1	-2	-2.12	0.94
O6	1	-2	-1.85	1.08
O7	1	-2	-2.05	0.97
O8	1	-2	-1.73	1.16
O9	1	-2	-1.90	1.05
O10	1	-2	-2.09	0.96
O11	1	-2	-1.92	1.04
O12	1	-2	-2.18	0.92
O13	1	-2	-2.06	0.97
O14	1	-2	-2.00	1.00
O15	1	-2	-1.98	1.01
O16	1	-2	-1.91	1.05
O17	1	-2	-2.05	0.98
O18	1	-2	-1.91	1.05
O19	1	-2	-2.09	0.96
O20	1	-2	-2.09	0.96
O21	1	-2	-2.12	0.94
O22	1	-2	-1.74	1.15
O23	1	-2	-2.05	0.97
O24	1	-2	-2.00	1.00

the polyhedra. Therefore the anionic charges of oxygen deviate slightly from the ideal value -2. This also explains the variation of cation–anion distances in the various polyhedra in the crystal structure of $\text{AgSr}_4\text{Cu}_{4.5}(\text{PO}_4)_6$.

The plausibility of a crystal-structure model may also be tested by the global instability index (GII) (Salinas-Sánchez *et al.*, 1992). The calculated value of the GII index measures the deviation of the bond-valence sums from the formal valence V_i averaged over all N atoms of the asymmetric unit. For an unstrained structure, GII is below 0.1 v.u. and may approach 0.2 v.u. in a structure with lattice-induced strains (Adams *et al.*, 2004). Values larger than 0.2 v.u. are typically taken as an indication of the presence of intrinsic strains strong enough to cause instability of the crystal structure (Brown, 1992). For the crystal structure of the title compound, $\text{GII} = 0.0944$, which indicates high stability and rigidity of the proposed structural model.

3. Database survey

A search in the ICSD database shows that no compounds are currently known in the quaternary system $\text{AgO}/\text{SrO}/\text{CuO}/\text{P}_2\text{O}_5$. The same is true within the $\text{AgO}/\text{SrO}/\text{P}_2\text{O}_5$ ternary system. However, one compound is known in the $\text{AgO}/\text{CuO}/\text{P}_2\text{O}_5$ ternary system, *viz.* $\beta\text{-AgCuPO}_4$ which crystallizes in the Pbca space group (Quarton & Oumba, 1983). There are seven compounds known in the ternary $\text{SrO}/\text{CuO}/\text{P}_2\text{O}_5$ system, *viz.* $\text{Sr}_{9.1}\text{Cu}_{1.4}(\text{PO}_4)_7$, $\text{Sr}_3\text{Cu}_3(\text{PO}_4)_4$ (Belik *et al.*, 2002; Effenberger, 1999), $\text{Sr}_{2.88}\text{Cu}_{3.12}(\text{PO}_4)_4$ (Karanović *et al.*, 2010), $\text{Sr}_5(\text{CuO}_2)_{0.333}(\text{PO}_4)_3$ (Kazin *et al.*, 2003), $\text{Sr}_2\text{Cu}(\text{PO}_4)_2$, $\text{SrCu}_2(\text{PO}_4)_2$ (Belik *et al.*, 2005) and $\text{SrCu}(\text{P}_2\text{O}_7)$ (Moqine *et al.*, 1993). There is no apparent relation between the structures

Table 3
Experimental details.

Crystal data	
Chemical formula	$\text{AgCu}_{4.50}\text{O}_{24}\text{P}_6\text{Sr}_4$
M_r	1314.08
Crystal system, space group	Triclinic, $P\bar{1}$
Temperature (K)	296
a, b, c (Å)	9.1070 (1), 9.1514 (1), 13.7259 (2)
α, β, γ (°)	97.498 (1), 98.303 (1), 110.875 (1)
V (Å ³)	1036.97 (2)
Z	2
Radiation type	Mo $K\alpha$
μ (mm ⁻¹)	16.22
Crystal size (mm)	0.30 × 0.27 × 0.21
Data collection	Bruker X8 APEXII
Diffractometer	Multi-scan (SADABS; Krause <i>et al.</i> , 2015)
Absorption correction	
T_{\min}, T_{\max}	0.496, 0.747
No. of measured, independent and observed [$I > 2\sigma(I)$] reflections	32671, 8573, 7465
R_{int}	0.028
(sin θ/λ) _{max} (Å ⁻¹)	0.806
Refinement	
$R[F^2 > 2\sigma(F^2)], wR(F^2), S$	0.028, 0.059, 1.03
No. of reflections	8573
No. of parameters	359
$\Delta\rho_{\text{max}}, \Delta\rho_{\text{min}}$ (e Å ⁻³)	4.05, -3.87

Computer programs: *APEX2* and *SAINT* (Bruker, 2009), *SHELXT2014/7* (Sheldrick, 2015a), *SHELXL2014/7* (Sheldrick, 2015b), *ORTEP-3* for Windows (Farrugia, 2012), *DIAMOND* (Brandenburg, 2006) and *pubCIF* (Westrip, 2010).

of these compounds and that of the title compound $\text{AgSr}_4\text{Cu}_{4.5}(\text{PO}_4)_6$.

4. Synthesis and crystallization

Single crystals of the title compound were obtained using the hydrothermal method with the following mixture of reagents: silver nitrate, strontium nitrate, metallic copper and 85wt% phosphoric acid in a proportion corresponding to the molar ratio Ag:Cu:Sr:P = 1:3:1:3. The hydrothermal reaction was conducted in a 23 mL Teflon-lined autoclave with 12 mL of distilled water under autogenous pressure. The vessel was heated to 473 K for 4 d. After being filtered off, washed with distilled water and dried in air, the reaction product consisted of a light-blue crystals in various forms corresponding to the title compound.

5. Refinement

Crystal data, data collection and structure refinement details are summarized in Table 3. The refinement of the occupation of all atom sites shows full occupancy and leads to the stoichiometric formula $\text{AgSr}_4\text{Cu}_{4.5}(\text{PO}_4)_6$. However, the difference-Fourier map shows two electron-density peaks of intensity 4.05 and -3.87 e Å⁻³ located at 0.63 and 0.59 Å from Ag1, respectively. These rather strong peaks could not be removed using a different integration strategy or another absorption model.

Acknowledgements

The authors thank the Unit of Support for Technical and Scientific Research (UATRS, CNRST) for the X-ray measurements and Mohammed V University, Rabat, Morocco, for financial support.

References

- Adams, S., Moretzki, O. & Canadell, E. (2004). *Solid State Ionics*, **168**, 281–290.
- Alhakmi, G., Assani, A., Saadi, M., Follet, C. & El Ammari, L. (2013). *Acta Cryst. E69*, i56.
- Assani, A., Saadi, M., Zriouil, M. & El Ammari, L. (2011). *Acta Cryst. E67*, i5.
- Badroud, L., Ouikerroum, J., Amenzou, H., Bensitel, M., Sadel, A. & Zahir, M. (2001). *Ann. Chim. Sci. Mat.* **26**, 6, 131–138.
- Belik, A. A., Azuma, M., Matsuo, A., Whangbo, M. H., Koo, H. J., Kikuchi, J., Kaji, T., Okubo, S., Ohta, H., Kindo, K. & Takano, M. (2005). *Inorg. Chem.* **44**, 6632–6640.
- Belik, A. A., Malakho, A. P., Lazoryak, B. I. & Khasanov, S. S. (2002). *J. Solid State Chem.* **163**, 121–131.
- Belik, A. A., Malakho, A. P., Pokholok, K. V., Lazoryak, B. I. & Khasanov, S. S. (2000). *J. Solid State Chem.* **150**, 159–166.
- Brandenburg, K. (2006). *DIAMOND*. Crystal Impact GbR, Bonn, Germany.
- Brown, I. D. (1977). *Acta Cryst. B33*, 1305–1310.
- Brown, I. D. (1978). *Chem. Soc. Rev.* **7**, 359–376.
- Brown, I. D. (1992). *Z. Kristallogr.* **199**, 255–272.
- Bruker (2009). *APEX2*, and *SAINT*. Bruker AXS Inc., Madison, Wisconsin, USA.
- Dross, T. & Glaum, R. (2004). *Acta Cryst. E60*, i58–i60.
- Effenberger, H. (1999). *J. Solid State Chem.* **142**, 6–13.
- Eon, J.-G. & Nespolo, M. (2015). *Acta Cryst. B71*, 34–47.
- Farrugia, L. J. (2012). *J. Appl. Cryst.* **45**, 849–854.
- Fu, J. (2014). *Mater. Lett.* **118**, 84–87.
- Hadrich, A., Lautié, A. & Mhiri, T. (2001). *Spectrochim. Acta Part A*, **57**, 1673–1681.
- Hidouri, M., Lajmi, B., Wattiaux, A., Fournés, L., Darriet, J. & Ben Amara, M. (2004). *J. Solid State Chem.* **177**, 55–60.
- Hoppe, R. (1979). *Z. Kristallogr.* **150**, 23–52.
- Hoppe, R., Voigt, S., Glaum, H., Kissel, J., Müller, H. P. & Bernet, K. (1989). *J. Less-Common Met.* **156**, 105–122.
- Jerbi, H., Hidouri, M. & Ben Amara, M. (2010). *J. Rare Earths*, **28**, 481–487.
- Jeżowska-Trzebiatowska, B., Mazurak, Z. & Lis, T. (1980). *Acta Cryst. B36*, 1639–1641.
- Karanović, L., Šutović, S., Poleti, D., Đorđević, T. & Pačevski, A. (2010). *Acta Cryst. C66*, i42–i44.
- Kasuga, T., Yamamoto, K., Tsuzuki, T., Nogami, M. & Abe, Y. (1999). *Mater. Res. Bull.* **34**, 10–11, 1595–1600.
- Kazin, P. E., Karpov, A. S., Jansen, M., Nuss, J. & Tretyakov, Y. D. (2003). *Z. Anorg. Allg. Chem.* **629**, 344–352.
- Khmiyas, J., Assani, A., Saadi, M. & El Ammari, L. (2013). *Acta Cryst. E69*, i50.
- Krause, L., Herbst-Irmer, R., Sheldrick, G. M. & Stalke, D. (2015). *J. Appl. Cryst.* **48**, 3–10.
- LeGeros, R. Z. & Tung, M. S. (1983). *Caries Res.* **17**, 419–429.
- Mentre, O., Abraham, F., Deffontaines, B. & Vast, P. (1994). *Solid State Ionics*, **72**, 293–299.
- Moqine, A., Boukhari, A., Elammar, L. & Durand, J. (1993). *J. Solid State Chem.* **107**, 368–372.
- Nespolo, M. (2016). *Acta Cryst. B72*, 51–66.
- Nespolo, M., Ferraris, G., Ivaldi, G. & Hoppe, R. (2001). *Acta Cryst. B57*, 652–664.

- Nespolo, M., Ferraris, G. & Ohashi, H. (1999). *Acta Cryst. B* **55**, 902–916.
- Nespolo, M. & Guillot, B. (2016). *J. Appl. Cryst.* **49**, 317–321.
- Ould Saleck, A., Assani, A., Saadi, M., Mercier, C., Follet, C. & El Ammari, L. (2015). *Acta Cryst. E* **71**, 813–815.
- Quarton, M. & Oumba, M. T. (1983). *Mater. Res. Bull.* **18**, 967–974.
- Salinas-Sánchez, A., García-Muñoz, J. L., Rodríguez-Carvajal, J., Saez-Puche, R. & Martínez, J. L. (1992). *J. Solid State Chem.* **100**, 201–211.
- Sheldrick, G. M. (2015a). *Acta Cryst. A* **71**, 3–8.
- Sheldrick, G. M. (2015b). *Acta Cryst. C* **71**, 3–8.
- Spek, A. L. (2009). *Acta Cryst. D* **65**, 148–155.
- Suzuki, T., Toriyama, M., Hosono, H. & Abe, Y. (1991). *J. Ferment. Bioeng.* **72**, 5, 384–391.
- Ternane, R., Ferid, M., Kbir-Ariguib, N. & Trabelsi-Ayedi, M. (2000). *J. Alloys Compd.* **308**, 83–86.
- Westrip, S. P. (2010). *J. Appl. Cryst.* **43**, 920–925.

supporting information

Acta Cryst. (2020). E76, 186-191 [https://doi.org/10.1107/S2056989020000109]

Crystal structure of silver strontium copper orthophosphate, $\text{AgSr}_4\text{Cu}_{4.5}(\text{PO}_4)_6$

Jamal Khmiyas, Elhassan Benhsina, Said Ouaatta, Abderrazzak Assani, Mohamed Saadi and Lahcen El Ammari

Computing details

Data collection: *APEX2* (Bruker, 2009); cell refinement: *SAINT* (Bruker, 2009); data reduction: *SAINT* (Bruker, 2009); program(s) used to solve structure: *SHELXT2014/7* (Sheldrick, 2015a); program(s) used to refine structure: *SHELXL2014/7* (Sheldrick, 2015b); molecular graphics: *ORTEP-3 for Windows* (Farrugia, 2012), *DIAMOND* (Brandenburg, 2006); software used to prepare material for publication: *publCIF* (Westrip, 2010).

Silver strontium copper orthophosphate

Crystal data

$\text{AgCu}_{4.50}\text{O}_{24}\text{P}_6\text{Sr}_4$	$Z = 2$
$M_r = 1314.08$	$F(000) = 1223$
Triclinic, $P\bar{1}$	$D_x = 4.209 \text{ Mg m}^{-3}$
$a = 9.1070 (1) \text{ \AA}$	Mo $K\alpha$ radiation, $\lambda = 0.71073 \text{ \AA}$
$b = 9.1514 (1) \text{ \AA}$	Cell parameters from 8573 reflections
$c = 13.7259 (2) \text{ \AA}$	$\theta = 2.4\text{--}35.0^\circ$
$\alpha = 97.498 (1)^\circ$	$\mu = 16.22 \text{ mm}^{-1}$
$\beta = 98.303 (1)^\circ$	$T = 296 \text{ K}$
$\gamma = 110.875 (1)^\circ$	Block, light blue
$V = 1036.97 (2) \text{ \AA}^3$	$0.30 \times 0.27 \times 0.21 \text{ mm}$

Data collection

Bruker X8 APEXII	32671 measured reflections
diffractometer	8573 independent reflections
Radiation source: fine-focus sealed tube	7465 reflections with $I > 2\sigma(I)$
Graphite monochromator	$R_{\text{int}} = 0.028$
φ and ω scans	$\theta_{\text{max}} = 35.0^\circ, \theta_{\text{min}} = 2.4^\circ$
Absorption correction: multi-scan (SADABS; Krause <i>et al.</i> , 2015)	$h = -14 \rightarrow 14$
$T_{\text{min}} = 0.496, T_{\text{max}} = 0.747$	$k = -12 \rightarrow 14$
	$l = -21 \rightarrow 20$

Refinement

Refinement on F^2	$w = 1/[\sigma^2(F_o^2) + (0.0206P)^2 + 3.8655P]$
Least-squares matrix: full	where $P = (F_o^2 + 2F_c^2)/3$
$R[F^2 > 2\sigma(F^2)] = 0.028$	$(\Delta/\sigma)_{\text{max}} = 0.001$
$wR(F^2) = 0.059$	$\Delta\rho_{\text{max}} = 4.05 \text{ e \AA}^{-3}$
$S = 1.03$	$\Delta\rho_{\text{min}} = -3.87 \text{ e \AA}^{-3}$
8573 reflections	Extinction correction: SHELXL-2018/3 (Sheldrick, 2015b), $F_c^* = kF_c[1 + 0.001xF_c^2\lambda^3/\sin(2\theta)]^{-1/4}$
359 parameters	Extinction coefficient: 0.00083 (7)
0 restraints	

Special details

Geometry. All esds (except the esd in the dihedral angle between two l.s. planes) are estimated using the full covariance matrix. The cell esds are taken into account individually in the estimation of esds in distances, angles and torsion angles; correlations between esds in cell parameters are only used when they are defined by crystal symmetry. An approximate (isotropic) treatment of cell esds is used for estimating esds involving l.s. planes.

Fractional atomic coordinates and isotropic or equivalent isotropic displacement parameters (\AA^2)

	<i>x</i>	<i>y</i>	<i>z</i>	$U_{\text{iso}}^*/U_{\text{eq}}$
Ag1	0.60647 (3)	0.58776 (4)	0.10399 (2)	0.02934 (7)
Sr1	0.28824 (3)	0.81800 (3)	0.01654 (2)	0.00676 (5)
Sr2	0.07030 (3)	0.54033 (3)	0.33636 (2)	0.00652 (5)
Sr3	0.63381 (3)	0.17215 (3)	0.32562 (2)	0.00823 (5)
Sr4	0.87164 (3)	0.85230 (3)	0.35406 (2)	0.00832 (5)
Cu1	0.000000	0.000000	0.000000	0.00876 (9)
Cu2	0.19756 (4)	0.43833 (4)	0.10393 (2)	0.00679 (6)
Cu3	0.17555 (4)	-0.05281 (4)	0.22039 (2)	0.00602 (6)
Cu4	0.35439 (4)	0.35727 (4)	0.32546 (2)	0.00693 (6)
Cu5	0.51284 (4)	0.24192 (4)	0.54770 (2)	0.00725 (6)
P1	-0.00318 (8)	0.17911 (8)	0.20922 (5)	0.00451 (11)
P2	0.93662 (8)	0.60245 (8)	0.11620 (5)	0.00507 (11)
P3	0.24288 (8)	0.92189 (8)	0.44052 (5)	0.00544 (11)
P4	0.44974 (8)	0.78964 (8)	0.23844 (5)	0.00542 (11)
P5	0.37042 (8)	0.20301 (8)	0.11200 (5)	0.00480 (11)
P6	0.69847 (8)	0.54683 (8)	0.45908 (5)	0.00475 (11)
O1	0.1628 (2)	0.3232 (2)	0.22180 (14)	0.0064 (3)
O2	0.0314 (2)	0.0493 (2)	0.25727 (15)	0.0091 (3)
O3	-0.1119 (2)	0.2403 (2)	0.26131 (15)	0.0093 (3)
O4	-0.0762 (2)	0.1176 (2)	0.09618 (14)	0.0092 (3)
O5	1.0559 (3)	0.5276 (3)	0.15350 (15)	0.0128 (4)
O6	0.8509 (3)	0.6235 (3)	0.20225 (15)	0.0112 (4)
O7	0.8129 (2)	0.4854 (2)	0.02384 (14)	0.0092 (4)
O8	1.0258 (3)	0.7603 (2)	0.08664 (15)	0.0116 (4)
O9	0.3837 (2)	1.0680 (2)	0.43059 (15)	0.0106 (4)
O10	0.2988 (2)	0.7963 (2)	0.48272 (14)	0.0089 (3)
O11	0.1335 (3)	0.9560 (3)	0.50496 (16)	0.0129 (4)
O12	0.1398 (2)	0.8387 (2)	0.33335 (13)	0.0065 (3)
O13	0.3714 (2)	0.9110 (2)	0.21547 (14)	0.0087 (3)
O14	0.6258 (2)	0.8917 (2)	0.28321 (16)	0.0107 (4)
O15	0.4209 (3)	0.6805 (2)	0.13724 (14)	0.0099 (4)
O16	0.3742 (2)	0.6848 (2)	0.31152 (14)	0.0089 (3)
O17	0.3381 (3)	0.3334 (2)	0.06366 (15)	0.0094 (4)
O18	0.4811 (3)	0.1406 (2)	0.06409 (16)	0.0108 (4)
O19	0.4412 (2)	0.2650 (2)	0.22584 (14)	0.0092 (4)
O20	0.2067 (2)	0.0587 (2)	0.09995 (14)	0.0070 (3)
O21	0.6559 (2)	0.6837 (2)	0.42809 (15)	0.0094 (3)
O22	0.8374 (3)	0.5349 (3)	0.41485 (16)	0.0160 (4)
O23	0.7430 (2)	0.5693 (2)	0.57441 (14)	0.0090 (3)

O24	0.5494 (2)	0.3884 (2)	0.42094 (14)	0.0083 (3)
-----	------------	------------	--------------	------------

Atomic displacement parameters (\AA^2)

	U^{11}	U^{22}	U^{33}	U^{12}	U^{13}	U^{23}
Ag1	0.01409 (12)	0.04266 (17)	0.03685 (16)	0.01756 (12)	0.00787 (11)	0.00447 (13)
Sr1	0.00637 (10)	0.00740 (10)	0.00765 (10)	0.00327 (8)	0.00283 (8)	0.00199 (8)
Sr2	0.00621 (10)	0.00615 (10)	0.00775 (10)	0.00271 (8)	0.00232 (8)	0.00124 (7)
Sr3	0.00784 (11)	0.00971 (10)	0.00884 (10)	0.00481 (9)	0.00298 (8)	0.00198 (8)
Sr4	0.00637 (11)	0.01015 (11)	0.01038 (10)	0.00413 (9)	0.00398 (8)	0.00341 (8)
Cu1	0.0054 (2)	0.0135 (2)	0.00640 (18)	0.00484 (17)	-0.00058 (15)	-0.00297 (16)
Cu2	0.00818 (15)	0.00827 (14)	0.00676 (13)	0.00519 (12)	0.00333 (11)	0.00329 (10)
Cu3	0.00630 (14)	0.00746 (13)	0.00649 (13)	0.00409 (11)	0.00282 (11)	0.00295 (10)
Cu4	0.00585 (14)	0.00973 (14)	0.00516 (12)	0.00403 (11)	0.00015 (10)	-0.00060 (10)
Cu5	0.00636 (14)	0.00897 (14)	0.00652 (13)	0.00391 (11)	0.00033 (11)	0.00019 (10)
P1	0.0042 (3)	0.0048 (3)	0.0052 (2)	0.0022 (2)	0.0016 (2)	0.0010 (2)
P2	0.0043 (3)	0.0056 (3)	0.0050 (2)	0.0017 (2)	0.0006 (2)	0.0011 (2)
P3	0.0046 (3)	0.0056 (3)	0.0058 (3)	0.0020 (2)	0.0006 (2)	0.0001 (2)
P4	0.0047 (3)	0.0063 (3)	0.0053 (3)	0.0024 (2)	0.0007 (2)	0.0012 (2)
P5	0.0042 (3)	0.0051 (3)	0.0054 (2)	0.0018 (2)	0.0018 (2)	0.0010 (2)
P6	0.0043 (3)	0.0060 (3)	0.0048 (2)	0.0024 (2)	0.0017 (2)	0.0016 (2)
O1	0.0043 (8)	0.0073 (8)	0.0071 (8)	0.0017 (6)	0.0007 (6)	0.0020 (6)
O2	0.0109 (9)	0.0090 (8)	0.0119 (8)	0.0065 (7)	0.0058 (7)	0.0056 (7)
O3	0.0081 (9)	0.0080 (8)	0.0137 (9)	0.0042 (7)	0.0056 (7)	0.0016 (7)
O4	0.0083 (9)	0.0128 (9)	0.0067 (8)	0.0059 (7)	-0.0001 (7)	-0.0005 (7)
O5	0.0156 (10)	0.0221 (11)	0.0095 (8)	0.0159 (9)	0.0041 (7)	0.0058 (8)
O6	0.0088 (9)	0.0165 (10)	0.0098 (8)	0.0063 (8)	0.0038 (7)	0.0011 (7)
O7	0.0097 (9)	0.0065 (8)	0.0071 (8)	-0.0004 (7)	-0.0015 (7)	0.0002 (6)
O8	0.0122 (10)	0.0079 (8)	0.0110 (9)	-0.0011 (7)	0.0034 (7)	0.0023 (7)
O9	0.0091 (9)	0.0083 (8)	0.0096 (8)	-0.0017 (7)	0.0013 (7)	0.0006 (7)
O10	0.0104 (9)	0.0114 (9)	0.0080 (8)	0.0072 (7)	0.0019 (7)	0.0038 (7)
O11	0.0112 (10)	0.0164 (10)	0.0120 (9)	0.0067 (8)	0.0040 (7)	-0.0004 (7)
O12	0.0061 (8)	0.0075 (8)	0.0052 (7)	0.0020 (7)	0.0002 (6)	0.0018 (6)
O13	0.0092 (9)	0.0110 (9)	0.0095 (8)	0.0069 (7)	0.0027 (7)	0.0043 (7)
O14	0.0063 (9)	0.0086 (8)	0.0157 (9)	0.0020 (7)	-0.0011 (7)	0.0032 (7)
O15	0.0102 (9)	0.0124 (9)	0.0073 (8)	0.0061 (7)	0.0005 (7)	-0.0014 (7)
O16	0.0084 (9)	0.0106 (8)	0.0069 (8)	0.0023 (7)	0.0011 (7)	0.0035 (6)
O17	0.0112 (9)	0.0090 (8)	0.0125 (9)	0.0063 (7)	0.0067 (7)	0.0055 (7)
O18	0.0102 (9)	0.0108 (9)	0.0152 (9)	0.0063 (7)	0.0077 (7)	0.0028 (7)
O19	0.0079 (9)	0.0128 (9)	0.0063 (8)	0.0051 (7)	-0.0007 (7)	-0.0018 (7)
O20	0.0049 (8)	0.0061 (8)	0.0081 (8)	0.0004 (6)	0.0001 (6)	0.0017 (6)
O21	0.0094 (9)	0.0088 (8)	0.0132 (9)	0.0048 (7)	0.0048 (7)	0.0063 (7)
O22	0.0108 (10)	0.0293 (12)	0.0141 (9)	0.0117 (9)	0.0087 (8)	0.0067 (9)
O23	0.0108 (9)	0.0137 (9)	0.0048 (7)	0.0076 (7)	0.0007 (7)	0.0015 (6)
O24	0.0068 (8)	0.0070 (8)	0.0095 (8)	0.0020 (7)	-0.0012 (7)	0.0007 (6)

Geometric parameters (\AA , ^\circ)

Ag1—O15	2.220 (2)	Cu2—O17	1.951 (2)
Ag1—O6	2.319 (2)	Cu2—O7 ⁱ	1.9723 (19)
Ag1—O17 ⁱ	2.565 (2)	Cu2—O1	2.0450 (19)
Ag1—O17	2.630 (2)	Cu2—O15	2.348 (2)
Ag1—O7	2.684 (2)	Cu3—O13 ^{vii}	1.936 (2)
Sr1—O18 ⁱ	2.449 (2)	Cu3—O2	1.948 (2)
Sr1—O7 ⁱ	2.5484 (19)	Cu3—O12 ^{vii}	1.9528 (18)
Sr1—O4 ⁱⁱ	2.580 (2)	Cu3—O20	2.0551 (19)
Sr1—O8 ⁱⁱⁱ	2.610 (2)	Cu3—O8 ^{xi}	2.225 (2)
Sr1—O15	2.615 (2)	Cu4—O23 ^v	1.914 (2)
Sr1—O13	2.6628 (19)	Cu4—O19	1.922 (2)
Sr1—O20 ^{iv}	2.7325 (19)	Cu4—O24	1.9553 (19)
Sr1—O18 ^{iv}	2.774 (2)	Cu4—O1	1.9866 (19)
Sr2—O5 ⁱⁱⁱ	2.480 (2)	Cu5—O21 ^v	1.942 (2)
Sr2—O22 ⁱⁱⁱ	2.502 (2)	Cu5—O10 ^v	1.959 (2)
Sr2—O23 ^v	2.517 (2)	Cu5—O16 ^v	1.9591 (19)
Sr2—O12	2.5813 (19)	Cu5—O9 ^{vii}	1.988 (2)
Sr2—O3	2.622 (2)	Cu5—O24	2.322 (2)
Sr2—O16	2.703 (2)	P1—O3	1.516 (2)
Sr2—O1	2.8087 (19)	P1—O2	1.535 (2)
Sr2—O10	2.819 (2)	P1—O4	1.541 (2)
Sr2—O6 ⁱⁱⁱ	2.890 (2)	P1—O1	1.581 (2)
Sr3—O3 ^{vi}	2.498 (2)	P2—O8	1.524 (2)
Sr3—O19	2.520 (2)	P2—O6	1.535 (2)
Sr3—O14 ^{vii}	2.529 (2)	P2—O5	1.540 (2)
Sr3—O10 ^v	2.5672 (19)	P2—O7	1.548 (2)
Sr3—O24	2.630 (2)	P3—O11	1.508 (2)
Sr3—O13 ^{vii}	2.766 (2)	P3—O9	1.525 (2)
Sr3—O9 ^{vii}	2.816 (2)	P3—O10	1.555 (2)
Sr3—O22	3.139 (3)	P3—O12	1.5572 (19)
Sr3—O11 ^v	3.511 (2)	P4—O14	1.523 (2)
Sr4—O11 ^{viii}	2.455 (2)	P4—O15	1.530 (2)
Sr4—O21	2.470 (2)	P4—O16	1.543 (2)
Sr4—O14	2.475 (2)	P4—O13	1.560 (2)
Sr4—O2 ^{ix}	2.539 (2)	P5—O18	1.509 (2)
Sr4—O12 ^{vi}	2.543 (2)	P5—O17	1.533 (2)
Sr4—O6	2.688 (2)	P5—O19	1.548 (2)
Sr4—O11 ^{vi}	2.707 (2)	P5—O20	1.570 (2)
Sr4—O22	3.048 (2)	P5—O1	2.988 (2)
Cu1—O4 ^x	1.9515 (19)	P6—O22	1.512 (2)
Cu1—O4	1.9515 (19)	P6—O21	1.529 (2)
Cu1—O20 ^x	2.0138 (19)	P6—O23	1.544 (2)
Cu1—O20	2.0138 (19)	P6—O24	1.553 (2)
Cu2—O5 ⁱⁱⁱ	1.912 (2)		
O15—Ag1—O6	130.30 (7)	O6—Sr4—O22	65.95 (6)

O15—Ag1—O17 ⁱ	104.15 (7)	O11 ^{vi} —Sr4—O22	80.99 (6)
O6—Ag1—O17 ⁱ	107.23 (7)	O4 ^x —Cu1—O4	180.0
O15—Ag1—O17	75.47 (7)	O4 ^x —Cu1—O20 ^x	90.19 (8)
O6—Ag1—O17	127.71 (7)	O4—Cu1—O20 ^x	89.82 (8)
O17 ⁱ —Ag1—O17	107.34 (5)	O4 ^x —Cu1—O20	89.82 (8)
O15—Ag1—O7	167.66 (7)	O4—Cu1—O20	90.18 (8)
O6—Ag1—O7	59.96 (6)	O20 ^x —Cu1—O20	180.0
O17 ⁱ —Ag1—O7	64.01 (6)	O4 ^x —Cu1—O8 ⁱ	104.34 (7)
O17—Ag1—O7	103.95 (6)	O4—Cu1—O8 ⁱ	75.66 (7)
O18 ⁱ —Sr1—O7 ⁱ	94.81 (7)	O20 ^x —Cu1—O8 ⁱ	65.34 (7)
O18 ⁱ —Sr1—O4 ⁱⁱ	108.26 (7)	O20—Cu1—O8 ⁱ	114.66 (7)
O7 ⁱ —Sr1—O4 ⁱⁱ	104.05 (6)	O4 ^x —Cu1—O8 ^{xi}	75.66 (7)
O18 ⁱ —Sr1—O8 ⁱⁱⁱ	174.83 (7)	O4—Cu1—O8 ^{xi}	104.34 (7)
O7 ⁱ —Sr1—O8 ⁱⁱⁱ	82.72 (7)	O20 ^x —Cu1—O8 ^{xi}	114.66 (7)
O4 ⁱⁱ —Sr1—O8 ⁱⁱⁱ	68.14 (7)	O20—Cu1—O8 ^{xi}	65.34 (7)
O18 ⁱ —Sr1—O15	86.11 (7)	O8 ⁱ —Cu1—O8 ^{xi}	180.00 (8)
O7 ⁱ —Sr1—O15	62.56 (6)	O5 ⁱⁱⁱ —Cu2—O17	174.10 (9)
O4 ⁱⁱ —Sr1—O15	161.76 (7)	O5 ⁱⁱⁱ —Cu2—O7 ⁱ	95.24 (9)
O8 ⁱⁱⁱ —Sr1—O15	96.71 (7)	O17—Cu2—O7 ⁱ	90.39 (8)
O18 ⁱ —Sr1—O13	113.18 (7)	O5 ⁱⁱⁱ —Cu2—O1	82.50 (8)
O7 ⁱ —Sr1—O13	107.77 (6)	O17—Cu2—O1	91.63 (8)
O4 ⁱⁱ —Sr1—O13	124.26 (6)	O7 ⁱ —Cu2—O1	168.00 (8)
O8 ⁱⁱⁱ —Sr1—O13	71.95 (6)	O5 ⁱⁱⁱ —Cu2—O15	95.57 (9)
O15—Sr1—O13	55.45 (6)	O17—Cu2—O15	87.46 (8)
O18 ⁱ —Sr1—O20 ^{iv}	124.05 (6)	O7 ⁱ —Cu2—O15	76.16 (7)
O7 ⁱ —Sr1—O20 ^{iv}	141.00 (6)	O1—Cu2—O15	115.74 (7)
O4 ⁱⁱ —Sr1—O20 ^{iv}	63.53 (6)	O5 ⁱⁱⁱ —Cu2—O8 ⁱ	97.38 (8)
O8 ⁱⁱⁱ —Sr1—O20 ^{iv}	58.28 (6)	O17—Cu2—O8 ⁱ	84.24 (8)
O15—Sr1—O20 ^{iv}	118.08 (6)	O7 ⁱ —Cu2—O8 ⁱ	56.67 (7)
O13—Sr1—O20 ^{iv}	62.82 (6)	O1—Cu2—O8 ⁱ	111.79 (7)
O18 ⁱ —Sr1—O18 ^{iv}	71.86 (7)	O15—Cu2—O8 ⁱ	131.91 (6)
O7 ⁱ —Sr1—O18 ^{iv}	163.91 (6)	O5 ⁱⁱⁱ —Cu2—O4	83.95 (8)
O4 ⁱⁱ —Sr1—O18 ^{iv}	89.03 (6)	O17—Cu2—O4	92.22 (7)
O8 ⁱⁱⁱ —Sr1—O18 ^{iv}	111.27 (6)	O7 ⁱ —Cu2—O4	113.28 (7)
O15—Sr1—O18 ^{iv}	106.49 (6)	O1—Cu2—O4	54.83 (6)
O13—Sr1—O18 ^{iv}	70.98 (6)	O15—Cu2—O4	170.55 (6)
O20 ^{iv} —Sr1—O18 ^{iv}	53.59 (6)	O8 ⁱ —Cu2—O4	57.36 (5)
O5 ⁱⁱⁱ —Sr2—O22 ⁱⁱⁱ	121.69 (7)	O13 ^{vii} —Cu3—O2	160.18 (9)
O5 ⁱⁱⁱ —Sr2—O23 ^v	116.94 (6)	O13 ^{vii} —Cu3—O12 ^{vii}	91.65 (8)
O22 ⁱⁱⁱ —Sr2—O23 ^v	115.45 (7)	O2—Cu3—O12 ^{vii}	88.14 (8)
O5 ⁱⁱⁱ —Sr2—O12	81.20 (7)	O13 ^{vii} —Cu3—O20	89.56 (8)
O22 ⁱⁱⁱ —Sr2—O12	89.49 (7)	O2—Cu3—O20	91.05 (8)
O23 ^v —Sr2—O12	124.57 (6)	O12 ^{vii} —Cu3—O20	178.46 (8)
O5 ⁱⁱⁱ —Sr2—O3	77.65 (7)	O13 ^{vii} —Cu3—O8 ^{xi}	96.00 (8)
O22 ⁱⁱⁱ —Sr2—O3	83.32 (7)	O2—Cu3—O8 ^{xi}	103.27 (9)
O23 ^v —Sr2—O3	84.85 (7)	O12 ^{vii} —Cu3—O8 ^{xi}	104.10 (8)
O12—Sr2—O3	149.55 (6)	O20—Cu3—O8 ^{xi}	74.82 (7)
O5 ⁱⁱⁱ —Sr2—O16	73.18 (7)	O13 ^{vii} —Cu3—O19	71.97 (7)

O22 ⁱⁱⁱ —Sr2—O16	152.12 (7)	O2—Cu3—O19	92.23 (7)
O23 ^v —Sr2—O16	68.53 (6)	O12 ^{vii} —Cu3—O19	126.04 (7)
O12—Sr2—O16	68.48 (6)	O20—Cu3—O19	55.29 (6)
O3—Sr2—O16	124.31 (6)	O8 ^{xi} —Cu3—O19	127.99 (6)
O5 ⁱⁱⁱ —Sr2—O1	58.77 (6)	O13 ^{vii} —Cu3—O9 ^{vii}	72.67 (7)
O22 ⁱⁱⁱ —Sr2—O1	137.87 (7)	O2—Cu3—O9 ^{vii}	91.22 (7)
O23 ^v —Sr2—O1	61.68 (6)	O12 ^{vii} —Cu3—O9 ^{vii}	54.82 (7)
O12—Sr2—O1	128.37 (6)	O20—Cu3—O9 ^{vii}	126.52 (7)
O3—Sr2—O1	54.80 (6)	O8 ^{xi} —Cu3—O9 ^{vii}	154.46 (7)
O16—Sr2—O1	69.52 (6)	O19—Cu3—O9 ^{vii}	71.23 (5)
O5 ⁱⁱⁱ —Sr2—O10	122.96 (7)	O23 ^v —Cu4—O19	175.03 (9)
O22 ⁱⁱⁱ —Sr2—O10	94.73 (7)	O23 ^v —Cu4—O24	94.12 (8)
O23 ^v —Sr2—O10	73.63 (6)	O19—Cu4—O24	86.62 (8)
O12—Sr2—O10	54.70 (6)	O23 ^v —Cu4—O1	89.30 (8)
O3—Sr2—O10	155.20 (6)	O19—Cu4—O1	90.03 (8)
O16—Sr2—O10	58.88 (6)	O24—Cu4—O1	176.54 (8)
O1—Sr2—O10	120.87 (6)	O23 ^v —Cu4—O16	70.33 (7)
O5 ⁱⁱⁱ —Sr2—O6 ⁱⁱⁱ	54.03 (6)	O19—Cu4—O16	114.25 (7)
O22 ⁱⁱⁱ —Sr2—O6 ⁱⁱⁱ	70.73 (6)	O24—Cu4—O16	104.78 (7)
O23 ^v —Sr2—O6 ⁱⁱⁱ	169.49 (6)	O1—Cu4—O16	75.83 (7)
O12—Sr2—O6 ⁱⁱⁱ	62.19 (6)	O23 ^v —Cu4—O2	87.24 (7)
O3—Sr2—O6 ⁱⁱⁱ	87.58 (6)	O19—Cu4—O2	88.45 (7)
O16—Sr2—O6 ⁱⁱⁱ	110.36 (6)	O24—Cu4—O2	128.42 (7)
O1—Sr2—O6 ⁱⁱⁱ	107.91 (6)	O1—Cu4—O2	52.25 (6)
O10—Sr2—O6 ⁱⁱⁱ	115.23 (6)	O16—Cu4—O2	123.74 (5)
O3 ^{vi} —Sr3—O19	110.38 (7)	O21 ^v —Cu5—O10 ^v	169.90 (9)
O3 ^{vi} —Sr3—O14 ^{vii}	82.58 (7)	O21 ^v —Cu5—O16 ^v	92.79 (9)
O19—Sr3—O14 ^{vii}	122.19 (6)	O10 ^v —Cu5—O16 ^v	87.76 (8)
O3 ^{vi} —Sr3—O10 ^v	108.90 (7)	O21 ^v —Cu5—O9 ^{vii}	97.24 (9)
O19—Sr3—O10 ^v	127.01 (6)	O10 ^v —Cu5—O9 ^{vii}	86.98 (9)
O14 ^{vii} —Sr3—O10 ^v	96.76 (6)	O16 ^v —Cu5—O9 ^{vii}	151.10 (9)
O3 ^{vi} —Sr3—O24	122.99 (6)	O21 ^v —Cu5—O24	87.84 (8)
O19—Sr3—O24	62.15 (6)	O10 ^v —Cu5—O24	83.75 (8)
O14 ^{vii} —Sr3—O24	152.48 (7)	O16 ^v —Cu5—O24	126.58 (8)
O10 ^v —Sr3—O24	67.04 (6)	O9 ^{vii} —Cu5—O24	80.99 (8)
O3 ^{vi} —Sr3—O13 ^{vii}	117.02 (6)	O21 ^v —Cu5—O23	91.10 (7)
O19—Sr3—O13 ^{vii}	70.32 (6)	O10 ^v —Cu5—O23	79.53 (7)
O14 ^{vii} —Sr3—O13 ^{vii}	54.77 (6)	O16 ^v —Cu5—O23	71.14 (7)
O10 ^v —Sr3—O13 ^{vii}	119.03 (6)	O9 ^{vii} —Cu5—O23	135.31 (7)
O24—Sr3—O13 ^{vii}	112.29 (6)	O24—Cu5—O23	55.44 (6)
O3 ^{vi} —Sr3—O9 ^{vii}	166.81 (6)	O21 ^v —Cu5—O14 ^v	70.52 (7)
O19—Sr3—O9 ^{vii}	82.79 (6)	O10 ^v —Cu5—O14 ^v	117.73 (7)
O14 ^{vii} —Sr3—O9 ^{vii}	90.80 (6)	O16 ^v —Cu5—O14 ^v	56.61 (7)
O10 ^v —Sr3—O9 ^{vii}	60.41 (6)	O9 ^{vii} —Cu5—O14 ^v	101.64 (7)
O24—Sr3—O9 ^{vii}	62.03 (6)	O24—Cu5—O14 ^v	158.36 (6)
O13 ^{vii} —Sr3—O9 ^{vii}	66.93 (6)	O23—Cu5—O14 ^v	122.40 (5)
O3 ^{vi} —Sr3—O22	73.38 (6)	O3—P1—O2	111.77 (11)
O19—Sr3—O22	86.10 (6)	O3—P1—O4	110.53 (12)

O14 ^{vii} —Sr3—O22	148.30 (6)	O2—P1—O4	110.81 (11)
O10 ^v —Sr3—O22	72.66 (6)	O3—P1—O1	107.91 (11)
O24—Sr3—O22	50.51 (6)	O2—P1—O1	107.36 (11)
O13 ^{vii} —Sr3—O22	156.23 (6)	O4—P1—O1	108.30 (11)
O9 ^{vii} —Sr3—O22	108.16 (6)	O8—P2—O6	112.23 (12)
O3 ^{vi} —Sr3—O11 ^v	78.24 (6)	O8—P2—O5	110.05 (13)
O19—Sr3—O11 ^v	170.75 (6)	O6—P2—O5	106.61 (12)
O14 ^{vii} —Sr3—O11 ^v	61.04 (6)	O8—P2—O7	109.64 (11)
O10 ^v —Sr3—O11 ^v	44.55 (6)	O6—P2—O7	109.63 (12)
O24—Sr3—O11 ^v	110.69 (5)	O5—P2—O7	108.57 (12)
O13 ^{vii} —Sr3—O11 ^v	109.31 (5)	O11—P3—O9	115.26 (12)
O9 ^{vii} —Sr3—O11 ^v	88.58 (6)	O11—P3—O10	107.09 (12)
O22—Sr3—O11 ^v	93.45 (6)	O9—P3—O10	112.23 (12)
O11 ^{viii} —Sr4—O21	77.94 (7)	O11—P3—O12	107.68 (12)
O11 ^{viii} —Sr4—O14	80.40 (7)	O9—P3—O12	107.88 (11)
O21—Sr4—O14	74.02 (7)	O10—P3—O12	106.25 (11)
O11 ^{viii} —Sr4—O2 ^{ix}	98.52 (7)	O14—P4—O15	114.18 (12)
O21—Sr4—O2 ^{ix}	163.95 (7)	O14—P4—O16	110.49 (11)
O14—Sr4—O2 ^{ix}	89.98 (7)	O15—P4—O16	108.08 (12)
O11 ^{viii} —Sr4—O12 ^{vi}	118.73 (7)	O14—P4—O13	104.92 (11)
O21—Sr4—O12 ^{vi}	130.97 (6)	O15—P4—O13	105.27 (11)
O14—Sr4—O12 ^{vi}	149.08 (7)	O16—P4—O13	113.93 (11)
O2 ^{ix} —Sr4—O12 ^{vi}	64.54 (6)	O18—P5—O17	113.12 (11)
O11 ^{viii} —Sr4—O6	174.63 (7)	O18—P5—O19	109.40 (12)
O21—Sr4—O6	96.83 (7)	O17—P5—O19	110.47 (11)
O14—Sr4—O6	97.07 (7)	O18—P5—O20	107.49 (11)
O2 ^{ix} —Sr4—O6	86.17 (6)	O17—P5—O20	108.67 (11)
O12 ^{vi} —Sr4—O6	65.64 (6)	O19—P5—O20	107.49 (11)
O11 ^{viii} —Sr4—O11 ^{vi}	65.85 (8)	O18—P5—O1	175.64 (9)
O21—Sr4—O11 ^{vi}	103.32 (7)	O17—P5—O1	70.46 (8)
O14—Sr4—O11 ^{vi}	145.70 (7)	O19—P5—O1	66.55 (8)
O2 ^{ix} —Sr4—O11 ^{vi}	89.13 (7)	O20—P5—O1	72.96 (8)
O12 ^{vi} —Sr4—O11 ^{vi}	56.15 (6)	O22—P6—O21	110.56 (12)
O6—Sr4—O11 ^{vi}	117.07 (6)	O22—P6—O23	109.07 (12)
O11 ^{viii} —Sr4—O22	111.04 (7)	O21—P6—O23	111.36 (11)
O21—Sr4—O22	52.59 (6)	O22—P6—O24	109.57 (13)
O14—Sr4—O22	118.68 (6)	O21—P6—O24	108.90 (11)
O2 ^{ix} —Sr4—O22	141.14 (6)	O23—P6—O24	107.32 (11)
O12 ^{vi} —Sr4—O22	79.02 (6)		

Symmetry codes: (i) $-x+1, -y+1, -z$; (ii) $-x, -y+1, -z$; (iii) $x-1, y, z$; (iv) $x, y+1, z$; (v) $-x+1, -y+1, -z+1$; (vi) $x+1, y, z$; (vii) $x, y-1, z$; (viii) $-x+1, -y+2, -z+1$; (ix) $x+1, y+1, z$; (x) $-x, -y, -z$; (xi) $x-1, y-1, z$.